

## New Transient Electrical Polarization Phenomenon in Sawtooth Superlattices

F. Capasso, S. Luryi, W. T. Tsang, C. G. Bethea, and B. F. Levine

*AT & T Bell Laboratories, Murray Hill, New Jersey 07974*

(Received 30 September 1983)

Theory and experimental evidence of a new transient polarization phenomenon, unique to sawtooth superlattices, are presented. This effect is the consequence of the lack of reflection symmetry in these structures and can be used for the implementation of a new class of high-speed, displacement current photodetectors.

PACS numbers: 73.40.Lq, 71.30.+d

Considerable research effort in recent years has concentrated on both the novel physical properties<sup>1-4</sup> and the device applications of quantum-well heterostructure superlattices.<sup>5,6</sup> Much less attention, however, has been devoted to the physics of multilayer graded-gap structures of the type shown in Fig. 1 (sawtooth superlattice), although some interesting device applications have been explored, such as rectifiers,<sup>7</sup> staircase solid-state photomultipliers,<sup>8</sup> and repeated velocity overshoot devices.<sup>9</sup>

The lack of planes of reflection symmetry in such materials, compared to conventional quantum-well superlattices with rectangular wells and barriers, can open the door to a number of exciting new effects. In this Letter we report for the first time on a novel and unique property of sawtooth superlattices, namely, the possibility of generating a transient macroscopic electrical polarization extending over many periods of the superlattice. This effect is a direct consequence of the above-mentioned lack of reflection symmetry in these structures.

The energy-band diagram of a sawtooth  $p$ -type superlattice is sketched in Fig. 1(a). The layer thicknesses are typically a few hundred angstroms and a suitable material is graded-gap  $\text{Al}_x\text{-Ga}_{1-x}\text{As}$ . The superlattice is sandwiched between two highly doped  $p^+$  contact regions.

Let us assume that electron-hole pairs are excited by a very short pulse as shown in Fig. 1(a). Electrons experience a high quasielectric field (typically  $\geq 10^5$  V/cm) due to the grading whereas the total force acting on holes is virtually negligible because of the valence band-edge lineup in  $p$ -type materials. Therefore electrons separate from holes and reach the low-gap side in a subpicosecond time ( $\leq 10^{-13}$  sec).<sup>10</sup> This sets up an electrical polarization in the sawtooth structure which results in the appearance of a voltage across the device terminals [Fig. 1(b)]. This macroscopic dipole moment and its associated voltage subsequently decay in time by a combina-

tion of (a) dielectric relaxation and (b) hole drift under the action of the internal electric field produced by the separation of electrons and holes.

The excess hole density decays by dielectric relaxation to restore a flat valence band (equipotential) condition, as illustrated in Fig. 1(c). Note that in this final configuration holes have redistributed to neutralize the electrons at the bottom of the wells. Thus also the net negative charge density on the low-gap side of the wells has decreased with the same time constant as the positive charge packet (the dielectric relaxation time).

Maxwell's dielectric relaxation time in a  $p$ -type material is given by

$$\tau_M = \epsilon / (epdv_p/dE), \quad (1)$$

where  $E$  is the electric field and  $v_p$  the velocity of holes. In the mobility regime  $v_p = \mu E$  and the decay of the charge density (expressed per unity area)  $\sigma$  is given by the well-known expression

$$\sigma(t) = \sigma_0 \exp(-ep\mu t/\epsilon). \quad (2)$$

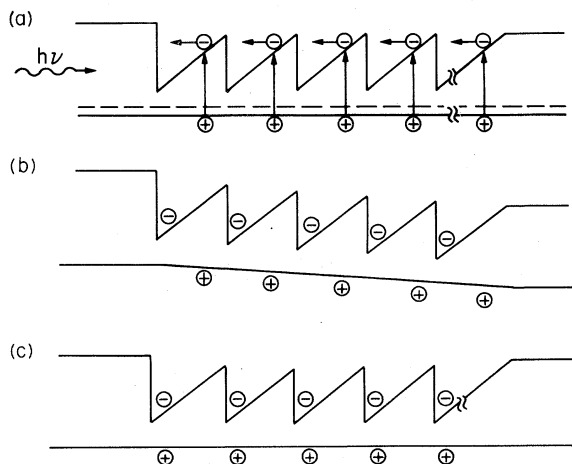


FIG. 1. Illustration of the formation and decay of the macroscopic electrical polarization in the superlattice structure.

The other mechanism by which the polarization decays is hole drift caused by the electric field created by the initial spatial separation of electrons and holes. One then has in the mobility regime

$$d(t) = d_0 - \int_0^t (\mu\sigma/\epsilon) dt', \quad (3)$$

where  $d(t)$  is the separation of the two charge packets and we have approximated these as thin sheets of uniform density  $\sigma$ .

In summary, the physical picture is that of two charge packets of opposite sign whose density decreases with time, due to dielectric relaxation, while their separation is reduced as a result of hole drift.

The time-dependent photovoltage across the device consisting of  $N$  layers can be written in the form

$$V(t) = N[\sigma(t)/\epsilon]d(t), \quad (4)$$

where  $\sigma$ 's in all the layers have been assumed for simplicity. (The more realistic case of non-uniform excitation can be considered by treating  $\sigma_0$  in Eq. (2) as a position-dependent quantity.) Substituting Eqs. (2) and (3) in Eq. (4) and integrating gives

$$V(t) = N \frac{\sigma_0 d_0}{\epsilon} \exp\left(\frac{-t}{\tau_M}\right) \times \left\{ 1 - \frac{\mu\sigma_0\tau_M}{\epsilon d_0} \left[ 1 - \exp\left(\frac{-t}{\tau_M}\right) \right] \right\}. \quad (5)$$

If  $\tau_M$  is much longer than the characteristic drift time  $t_d = d_0\epsilon/\mu\sigma_0$  then Eq. (5) reduces to

$$V(t) = (N\sigma_0 d_0/\epsilon)(1 - t/t_d). \quad (6)$$

In the opposite limit of  $\tau_M \ll t_d$  one has instead

$$V(t) = (N\sigma_0 d_0/\epsilon) \exp(-t/\tau_M). \quad (7)$$

In this case our device behaves as a plane capacitor ( $C = \epsilon S/l$ ) discharging through a leakage resistance [ $R = (1/ep\mu)l/S$ , where  $l$  is the thickness of the superlattice and  $S$  the device area]. Note that the  $RC$  time constant of this capacitor is simply the dielectric relaxation time  $\tau_M = \epsilon/ep\mu$ . In the case of an external load  $R_L$ , Eqs. (5)–(7) can be easily modified by inserting

$$\tau^{-1} = \tau_M^{-1} + 1/R_L C \quad (8)$$

in place of  $1/\tau_M$  in Eq. (5). In this case the time decay of the photovoltage is not only due to the above mechanisms but also to charge redistribution between the capacitance terminals via the load.

From (5) we can estimate the peak photovoltages obtainable from this polarization effect. For injected carrier densities in the range  $10^{10}$ – $10^{11}/\text{cm}^2$ ,  $d_0 \cong 500 \text{ \AA}$ , and  $N=5$ , we obtain photovoltages in the 30–300-mV range.

The dielectric relaxation time in the mobility regime varies from 1 to 500 ps in the doping range  $10^{17} \geq p \geq 10^{14}/\text{cm}^3$ . The characteristic hole drift time  $t_d$  is  $\geq 5$  ps for  $\sigma_0/e \leq 5 \times 10^{10}/\text{cm}^2$ . At higher injected carrier densities the internal electric field  $\sigma_0/\epsilon$  exceeds  $5 \times 10^3 \text{ V/cm}$  so that we are no more in the mobility regime and Eq. (5) loses its validity. In the saturated drift-velocity limit,  $v_p = v_{\text{sat}}$ , there is no dielectric relaxation ( $\tau_M = \infty$ ) and the photovoltage decays exclusively through the drift mechanism, expressed by Eq. (6) where now  $t_d = d_0/v_{\text{sat}}$ . These estimates indicate that the characteristic time scale of the transient polarization can be widely varied from 1 ps to several hundred picoseconds by changing the doping level and the injected charge density. Obviously this effect can be used to make a high-speed photovoltaic detector.

It should be pointed out that the minority-carrier lifetime plays no role in this phenomenon provided that (a) electrons have sufficiently long lifetimes to equilibrate in the conduction band and (b) the density of electrons collected in the wells is sufficiently low that quantization effects can be neglected. If these two conditions are satisfied, recombination of an electron with a hole clearly does not change the charge density  $\sigma$  or the separation of the charge packets  $d$ , thus leaving the photovoltage unaffected. The equilibration time of an electron in the conduction band is in the order of a few energy relaxation times ( $\tau_E \lesssim 1$  ps); and  $\tau_E$  is usually significantly smaller than the minority-carrier lifetime so that the first condition is generally satisfied. If the electron density is high enough for quantization effects to become important, then the spatial distribution of electrons in the wells will change as the density changes because of recombination thus affecting the size of the macroscopic polarization and the photovoltage. It is thus clear from these considerations that the structure of the superlattice and the level of photoexcitation will determine whether the observed effect is dependent or not on the minority-carrier lifetime.

The graded-gap superlattice structure shown in Fig. 1(a) was grown by molecular-beam epitaxy. A buffer layer of  $p^+$ -GaAs ( $\approx 1.0 \text{ \mu m}$ ) doped with Be to  $\approx 5 \times 10^{18} \text{ cm}^{-3}$  was first grown on a high-quality Zn-doped ( $\approx 4 \times 10^{18} \text{ cm}^{-3}$ ) (100) GaAs sub-

strate. This was then followed by the multilayer structure shown in Fig. 1(a). A total of ten graded periods were grown with a period of  $\approx 500 \text{ \AA}$ . The layers are graded from GaAs to  $\text{Al}_{0.2}\text{Ga}_{0.8}\text{As}$ . Since the graded period is only about  $500 \text{ \AA}$  and the grading is one sided with the opposite side abrupt, such grading cannot be easily achieved by ramping the temperature of the Al or Ga ovens. Instead, we achieved such unidirectional grading by controlling the speed with which the shutter closed the orifice of the Al effusion cell while maintaining the oven temperature constant. The Al flux intensity arriving at the substrate surface depends on the size of the Al orifice. The abrupt side of the period was accomplished by closing the Al cell abruptly, while the graded side was accomplished by closing the cell at discrete steps. Different wafers were grown with different Be concentrations ( $10^{15}$ – $10^{17}/\text{cm}^3$ ) in the superlattice region. A heavily doped GaAs layer of  $\approx 700 \text{ \AA}$  was grown on top of the  $\text{Al}_{0.45}\text{Ga}_{0.55}\text{As}$   $1\text{-}\mu\text{m}$ -thick ( $p \approx 5 \times 10^{18}/\text{cm}^3$ ) window layer to facilitate the formation of Ohmic contact. Ring-shaped Ohmic contacts were applied to the top and bottom of the structure by alloying plated AuZn. The portion of the thin, top, highly doped GaAs contact layer not covered by the metallization was then removed by a selective etch. The final devices were defined by mesa etching and had an area of  $2.7 \times 10^{-4} \text{ cm}^2$ . They were subsequently mounted in a  $50\text{-}\Omega$  microwave strip-line package coupled to a sampling scope. No external bias was applied to the devices.

The experiment consists in detecting a voltage pulse when the device is illuminated by a short light pulse. The source was a mode-locked dye laser with pulse width of  $\approx 4 \text{ ps}$  and a repetition rate of  $86 \text{ MHz}$ ; the wavelength ( $\lambda \approx 6400 \text{ \AA}$ ) is chosen so that it is transparent to the band gap of the window layer. The absorption length was estimated to be  $\approx 3500 \text{ \AA}$  by the averaging of recent absorption measurements in  $\text{Al}_x\text{Ga}_{1-x}\text{As}$  over the alloy composition  $x$ .<sup>11</sup> The peak power was  $\approx 1 \text{ W}$ .

Figure 2 shows the voltage pulse appearing across the device terminals. In this particular wafer the carrier concentration was  $\approx 10^6/\text{cm}^3$ . Note that the rise time is scope limited while the fall time (at the  $1/e$  point) is  $\approx 200 \text{ ps}$ . The observed pulse is not due to a possible Schottky-barrier diode caused by a nonperfect Ohmic contact, since the window layer is transparent to the incident light. Nevertheless, this was ruled out by checking out the  $IV$  characteristics of the

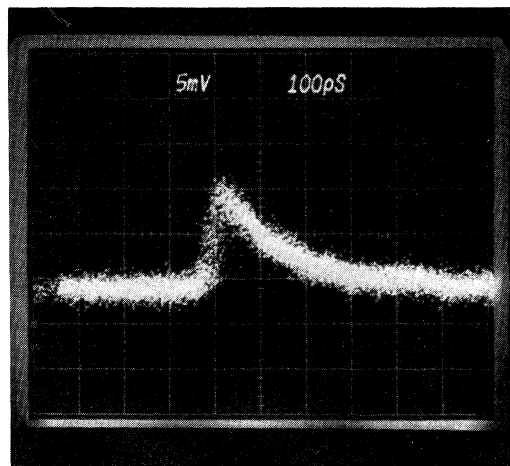


FIG. 2. Pulse response of one of the units to a 4-ps laser pulse.

device over a wide current range. Perfect linearity over several orders of magnitude up to  $100 \text{ mA}$  was found with a total series resistance of  $\approx 7 \text{ }\Omega$ . In addition superlattices with  $p$ -type rectangular quantum wells and barriers having the same layer thicknesses were also tested. No voltage pulse was detected in this case which is expected since no macroscopic electrical polarization can be created in such a structure by light absorption.

It was found that the fall time is sensitive to the background doping, as expected from the previous considerations. However, our pulse response cannot be quantitatively compared to Eq. (5). The reason is that the charge density  $\sigma$  is position dependent because of the obviously nonuniform optical excitation of the structure. In addition, in the layers with the highest density, the internal electric field due to the polarization may be approaching  $10^4 \text{ V/cm}$  and space-charge effects are present. As a consequence the dielectric relaxation time in these layers becomes significantly longer than in the mobility regime, dependent on the charge density and thus on the position inside the device. The problem then becomes strongly nonlinear and difficult to treat. In this case a general approach to the problem can be made via the impulsive impedance method used by Shockley in studying the transient voltage response of unipolar structures.<sup>12</sup>

As a final check on the experiment we found that our structure does not respond to a constant dc light signal. This is expected since the sawtooth structure of Fig. 1(a) cannot produce a dc

photoresponse. Unlike conventional semiconductor photodiode and photoconductive detectors, the current carried in this photodetector is of displacement rather than conduction nature since it is associated with a time-varying polarization. This current by continuity equals the conduction current in the external load.

In conclusion, theory and experimental evidence of a new polarization phenomenon in sawtooth superlattices has been presented. This effect represents a manifestation of the lack of reflection symmetry and can be used for the detection of fast light pulses.

We acknowledge the expert technical assistance of A. L. Hutchinson in the processing of the diodes.

---

<sup>1</sup>L. Esaki and L. L. Chang, *Phys. Rev. Lett.* **33**, 495 (1974).

<sup>2</sup>R. Dingle, A. C. Gossard, and W. Wiegmann, *Phys. Rev. Lett.* **34**, 1327 (1975).

<sup>3</sup>E. E. Mendez, L. L. Chang, G. Landgen, R. Ludeke,

and L. Esaki, *Phys. Rev. Lett.* **46**, 1230 (1981).

<sup>4</sup>L. L. Chang, N. Kaiwai, G. A. Sai-Halasz, R. Ludeke, and L. Esaki, *Appl. Phys. Lett.* **35**, 939 (1979).

<sup>5</sup>W. T. Tsang, *Appl. Phys. Lett.* **39**, 786 (1981).

<sup>6</sup>F. Capasso, W. T. Tsang, A. L. Hutchinson, and G. F. Williams, *Appl. Phys. Lett.* **40**, 38 (1982).

<sup>7</sup>C. L. Allyn, A. C. Gossard, and W. Wiegmann, *Appl. Phys. Lett.* **36**, 373 (1980).

<sup>8</sup>F. Capasso, W. T. Tsang, and G. F. Williams, *IEEE Trans. Electron Devices* **30**, 381 (1983).

<sup>9</sup>J. A. Cooper, F. Capasso, and K. K. Thornber, *IEEE Electron Devices Lett.* **3**, 497 (1982); F. Capasso, *J. Vac. Sci. Technol. B* **1**, 457 (1983).

<sup>10</sup>Recently a high steady-state electron velocity ( $2 \times 10^7$  cm/sec) has been directly measured in graded-gap  $p^+$ -AlGaAs in a quasielectric field of  $\approx 10^4$  kV/cm over a distance of  $0.4 \mu\text{m}$  [B. F. Levine, C. G. Bethea, W. T. Tsang, F. Capasso, K. K. Thornber, R. C. Fulton, and D. A. Kleinman, *Appl. Phys. Lett.* **42**, 769 (1983)]. In the present sawtooth superlattice, the electron velocity is expected to be significantly greater ( $\geq 5 \times 10^7$  cm/sec) since the layer thickness is considerably shorter, so that transient effects are important. Thus electrons move to the other end of the well in a time  $\leq 10^{-13}$  sec.

<sup>11</sup>D. Aspnes, private communication.

<sup>12</sup>W. Shockley, *Bell Syst. Tech. J.* **33**, 799 (1954).

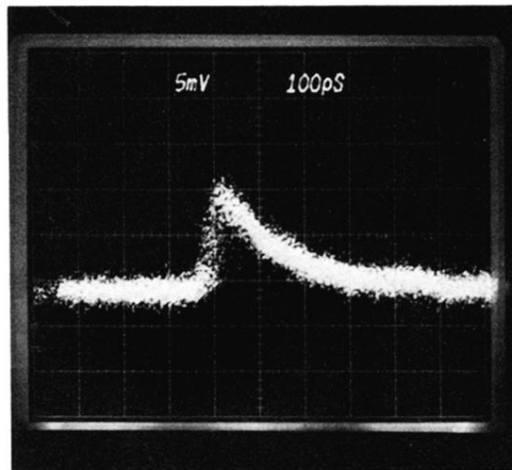


FIG. 2. Pulse response of one of the units to a 4-ps laser pulse.